Volume 43 | Number 15 | 21 April 2014 | Pages 5605–5936

Dalton Transactions

An international journal of inorganic chemistry

www.rsc.org/dalton

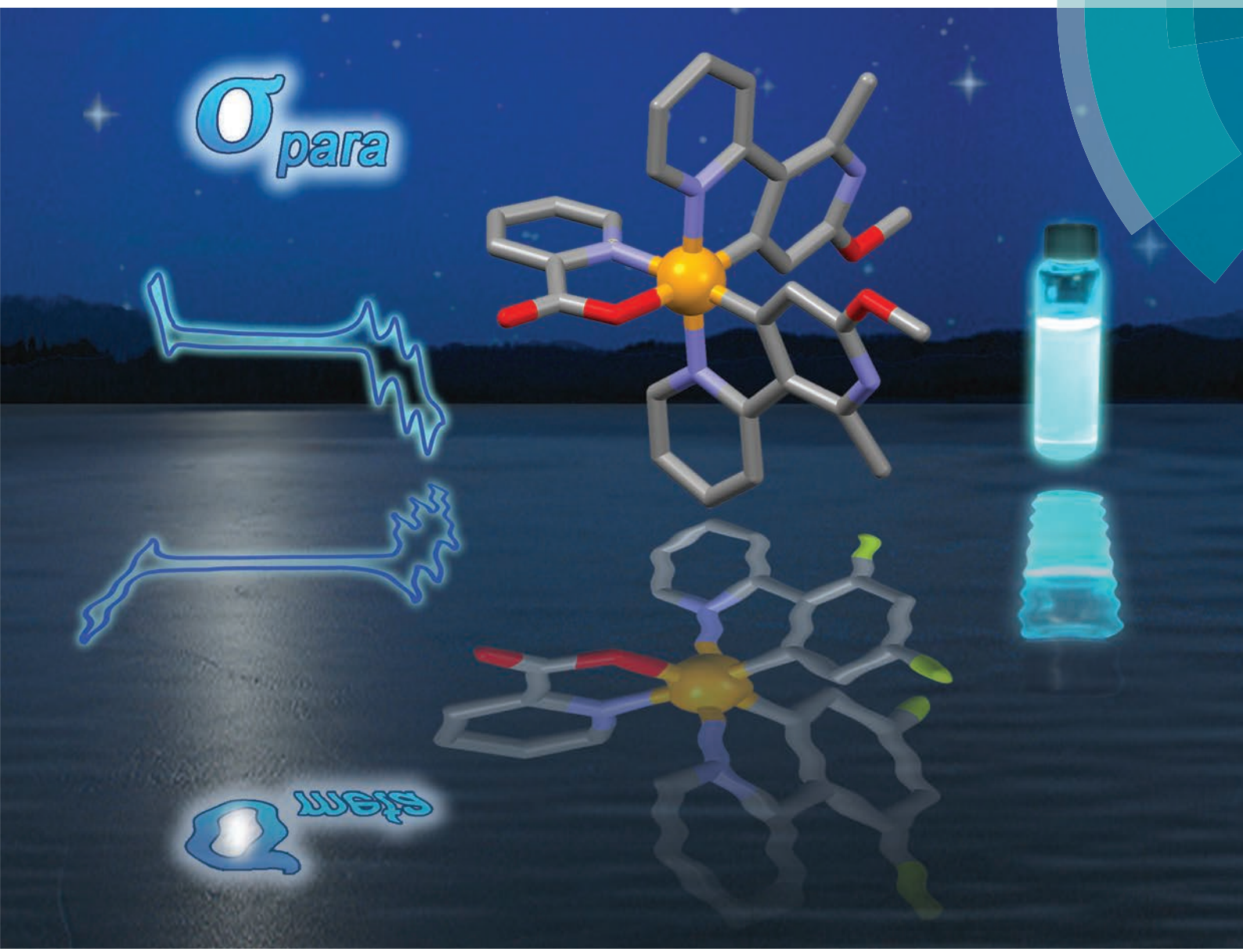

ISSN 1477-9226

ROYAL SOCIETY OF CHEMISTRY

COVER ARTICLE

Baranoff *et al.*

Structure–property relationships based on Hammett constants in cyclometalated iridium(III) complexes: their application to the design of a fluorine-free FIrPic-like emitter

Dalton Transactions

PAPER

View Article Online
View Journal | View Issue

Cite this: *Dalton Trans.*, 2014, **43**, 5667

Structure–property relationships based on Hammett constants in cyclometalated iridium(III) complexes: their application to the design of a fluorine-free FIrPic-like emitter†

Julien Frey,[a] Basile F. E. Curchod,[b] Rosario Scopelliti,[a] Ivano Tavernelli,[b] Ursula Rothlisberger,[b] Mohammad K. Nazeeruddin[a] and Etienne Baranoff*[c]

Received 1st October 2013,
Accepted 29th November 2013

DOI: 10.1039/c3dt52739e

www.rsc.org/dalton

While phosphorescent cyclometalated iridium(III) complexes have been widely studied, only correlations between oxidation potential E_{OX} and Hammett constant σ, and between the redox gap ($\Delta E_{REDOX} = E_{OX} - E_{RED}$) and emission or absorption wavelength (λ_{abs}, λ_{em}) have been reported. We present now a quantitative model based on Hammett parameters that rationalizes the effect of the substituents on the properties of cyclometalated iridium(III) complexes. This simple model allows predicting the apparent redox potentials as well as the electrochemical gap of homoleptic complexes based on phenylpyridine ligands with good accuracy. In particular, the model accounts for the unequal effect of the substituents on both the HOMO and the LUMO energy levels. Consequently, the model is used to anticipate the emission maxima of the corresponding complexes with improved reliability. We demonstrate in a series of phenylpyridine emitters that electron-donating groups can effectively replace electron-withdrawing substituents on the orthometallated phenyl to induce a blue shift of the emission. This result is in contrast with the common approach that uses fluorine to blue shift the emission maximum. Finally, as a proof of concept, we used electron-donating substituents to design a new fluorine-free complex, referred to as **EB343**, matching the various properties, namely oxidation and reduction potentials, electrochemical gap and emission profile, of the standard sky-blue emitter **FIrPic**.

Introduction

Comprehensive structure–properties relationships for transition metal complexes are essential owing to their great importance in catalysis, optoelectronics and sensing applications.[1–6] Among the many families of complexes of interest, cyclometalated iridium(III) complexes possess unique photophysical properties, namely high phosphorescence quantum yields and a relatively short triplet excited state lifetime.[7–13] As a result of these characteristics, they have attracted considerable interest for use as dopants in organic light-emitting diodes (OLEDs)[14–22] and virtually any application requiring highly phosphorescent materials.[23–31]

Interestingly the emission wavelength of iridium(III) complexes can be tuned over the entire visible spectrum. This color tuning is possible because, first, the emission is mainly a lowest unoccupied molecular orbital (LUMO) to highest occupied molecular orbital (HOMO) transition.[32] It is therefore possible to adjust the color of the emission by changing the HOMO–LUMO gap, which can be achieved simply by changing the ligand skeleton.[33–38] Second, the HOMO and LUMO are spatially differentiated.[32,39,40] For example, on complexes featuring 2-phenylpyridine (ppy) as a ligand, the HOMO is predominantly localized across the phenyl ring and the iridium center, whereas the LUMO resides preferentially on the pyridine.[32] In this case, the HOMO–LUMO gap can be tuned by grafting substituents onto the ligand skeleton and, depending on the position of the substituents, they will impact the LUMO or the HOMO energy levels. The substituents can exert both inductive and mesomeric effects that result in an electron-

[a]*Laboratory of Photonics and Interfaces, Institute of Chemical Sciences and Engineering, École Polytechnique Fédérale de Lausanne, CH-1015 Lausanne, Switzerland*
[b]*Laboratory of Computational Chemistry and Biochemistry, Institute of Chemical Sciences and Engineering, École Polytechnique Fédérale de Lausanne, CH-1015 Lausanne, Switzerland*
[c]*School of Chemistry, University of Birmingham, Edgbaston, Birmingham B15 2TT, UK. E-mail: e.baranoff@bham.ac.uk*

†Electronic supplementary information (ESI) available: Synthetic procedures, X-ray crystallographic data, additional figures, theoretical calculation, voltammograms, ^{1}H NMR and ^{19}F NMR spectra, and HRMS of the complexes. CCDC complex **1**: 964310, complex **2**: 964311, complex **3**: 964312, complex **4**: 964313, complex **6**: 964314, complex **7**: 964315. For ESI and crystallographic data in CIF or other electronic format see DOI: 10.1039/c3dt52739e

donating or withdrawing character. The electronic character of the substituents is quantified in terms of position according to Hammett σ-values (σ_{meta} or σ_{para}).[41] More positive (negative) values of σ are associated with the more electron-withdrawing (donating) substituent.[42] Hence acceptor (donor) groups are expected to stabilize (destabilize) the orbital that is involved by pulling out (pushing in) electron density from (to) this orbital, respectively. Hammett parameters have been paramount for the development of quantitative structure–property relationships (QSPR).[43] In general, it is possible to build strong QSPR between the nature of these substituents based on their Hammett σ-values and the corresponding electrochemical properties of series of compounds, and one can observe a linear dependence of oxidation (E_{OX}) or reduction (E_{RED}) potentials with respect to the Hammett parameters.[1–3,5,44–48]

For cyclometalated iridium(III) complexes, although there are reports on the correlation between oxidation potential E_{OX} and σ,[7,50] as well as the correlation between the redox gap ($\Delta E_{REDOX} = E_{OX} - E_{RED}$) and absorption or emission wavelength (λ_{abs}, λ_{em}),[50,51] there is apparently no general correlation between λ_{em} and Hammett σ-values. The early work of Watts and coworkers nicely illustrates these two paradigms.[49] The authors reported the electrochemical and photophysical data of a series of homologous homoleptic tris-cyclometalated iridium complexes [Ir(R-ppy)$_3$], ppy = 2-phenylpyridine and substituents on the phenyl R = H, 4-methyl, 4-propyl, 4-*tert*-butyl, 4-fluoro, 4-trifluoromethyl, 4-methoxy, 5-methoxy. The correlations of the Hammett parameters σ with the oxidation potentials E_{OX} and with the emission maxima λ_{em} are shown in Fig. S1† (experimental data are given in Table 1). Whereas the first correlation appears very convincing, the latter correlation with λ_{em} presents large discrepancies for the complexes [Ir(4-CF$_3$-ppy)$_3$] and [Ir(5-OMe-ppy)$_3$]. The trifluoromethyl substituent, a stronger acceptor than fluorine, results in green emission similar to the parent complex [Ir(ppy)$_3$], while the methoxy substituent, usually considered as an electron-donating group, results in red or blue shifted emission compared to [Ir(ppy)$_3$], depending on its position.

The oxidation potentials of cyclometalated iridium complexes can be related to the corresponding HOMO energy levels.[50,52] Since correlations between E_{OX} and σ-values seem reasonable, one can legitimately assume that the HOMO energy level and σ also correlate. For Ir(4-CF$_3$-ppy)$_3$, the HOMO level is shifted positively compared to Ir(ppy)$_3$ in agreement with the electron-withdrawing nature of the –CF$_3$ group. Consequently, the absence of an emission wavelength shift between those two complexes can be attributed to significant stabilization of the LUMO energy level in Ir(4-CF$_3$-ppy)$_3$ compared to Ir(ppy)$_3$. This implies that despite being located on the cyclometalated phenyl ring where the HOMO is mainly localized, the –CF$_3$ group also impacts the LUMO energy level of the complex. A thorough comparison of the –CF$_3$ and –F substituents reported by Avilov *et al.* also stresses the importance of the position of the substituents.[53] Based on a detailed theoretical analysis, the authors illustrate how the emission properties of bis-cyclometalated iridium complexes are influenced by the substitution pattern and conclude that both HOMO and LUMO energy levels are unequally impacted by those changes. This result about the position of the substituents is reminiscent of the effect of the methoxy group in the report of Watts, although this qualitative information is of limited assistance for practical design. Clearly, QSPR that would relate the electronic character of the substituents to the emissive property of the complex is still missing for cyclometalated iridium complexes.

We recently reported our initial progress towards such QSPR in an homologous series of halogen substituted bis-cyclometalated complexes [Ir(2-(2,4-diX-phenyl)pyridine)(pic)], with X = H, F (**FIrPic**), Cl, Br and pic = picolinate. We were able to link the Hammett parameters of the substituents to the wavelength of emission maxima.[54] Despite the higher values of σ_m for chlorine and bromine compared to fluorine, the emissions of the chloro and bromo substituted complexes are red-shifted with respect to **FIrPic**. Nevertheless, we obtained a very good correlation of σ_m *versus* E_{OX} along the series, as expected. To obtain a convincing correlation with λ_{em}, it was necessary to introduce the Hammett parameter that accounts for the substituents effect in *ortho*/*para* position, σ_p ($\approx \sigma_o$). The new relation ($\sigma_m - \sigma_p$) *versus* λ_{em} provided a quasi-quantitative rationalization of the unexpected shift of emission along the series: the chloride and bromide substituents (σ_p = 0.22) are much stronger electron-withdrawing elements towards the *para* position than the fluoride substituent (σ_p = 0.06) and therefore –Cl and –Br stabilize the LUMO, which is mainly localized on the pyridine ring that is in the *ortho*/*para* position of the substituents, much more than –F. This energetic stabilization of the LUMO has been reproduced with theoretical calculations.

We report now a quantitative model based on Hammett parameters that rationalizes the effect of the substituents on the properties of cyclometalated iridium(III) complexes. This model allows for predicting the apparent redox potentials as well as the electrochemical gap of complexes based on phenylpyridine ligands with good accuracy. In particular, the model accounts for the unequal effect of the substituents on both the HOMO and the LUMO energy levels. Consequently, the model can also be used to anticipate the emission maxima

Table 1 Experimental data from ref. 49 (λ_{em} at 77 K), values of the Hammett parameters[41] and the condition on the Hammett parameters according to eqn (12) and (13) (see below)

Complex	λ_{em} (nm)	λ_{em} (cm^{-1})	E_{OX}	σ_m	σ_p	Condition
Ir(ppy)$_3$	494	20 243	0.77	0	0	0.00
Ir(4-Me-ppy)$_3$	493	20 284	0.70	−0.07	−0.17	0.05
Ir(4-Pr-ppy)$_3$	496	20 161	0.67	−0.07	−0.15	0.03
Ir(4-*t*Bu-ppy)$_3$	497	20 121	0.66	−0.10	−0.20	0.04
Ir(4-F-ppy)$_3$	468	21 368	0.97	0.34	0.06	0.30
Ir(4-CF$_3$-ppy)$_3$	494	20 243	1.08	0.43	0.54	0.05
Ir(4-OMe-ppy)$_3$	481	20 790	0.75	0.12	−0.27	0.31
Ir(5-OMe-ppy)$_3$	539	18 553	0.55	0.12	−0.27	−0.35

of the corresponding complexes with improved reliability. Importantly, this model provides an improved theoretical frame that can help in further developing iridium emitters. In particular, we demonstrate in a series of phenylpyridine emitters that electron-donating groups can effectively replace electron-withdrawing substituents on the orthometallated phenyl to induce a blue shift of the emission. This result is in contrast with the common approach that uses fluorine to blue shift the emission maximum.

Finally, as a proof of concept, we used electron-donating substituents to design a new fluorine-free complex, referred to as **EB343**, matching the various properties, namely oxidation and reduction potentials, electrochemical gap and emission profile, of the standard sky-blue emitter **FIrPic**.

Experimental

Materials and general considerations

All materials and solvents were of reagent quality and used as received. $[Ir(COD)Cl]_2$ was purchased from Strem, $IrCl_3{\cdot}xH_2O$ from Heraeus, 2-phenylpyridine from Aldrich, and acetylacetone and picolinic acid from Fluka. **1**, **2**, and **FIrPic** were synthesized as previously reported.[54,55] ^1H and ^{13}C NMR spectra were recorded using a Bruker AV 400 MHz spectrometer. Chemical shifts δ (in ppm) are referenced to residual solvent peaks. ^{19}F NMR spectra were recorded using a Bruker AV 200 MHz spectrometer. Coupling constants are expressed in hertz (Hz). High-resolution mass spectra (HRMS) and elemental analyses have been performed by the Service d'Analyse of EPFL. UV-visible spectra were recorded in a 1 cm path length quartz cell on a Cary 100 spectrophotometer. Emission spectra were recorded on a Fluorolog 3-22 using a 90° optical geometry. Voltammetric measurements employed a PC controlled AutoLab PSTAT10 electrochemical workstation and were carried out in an argon-filled glove box, oxygen and water <5 ppm. All experiments were realized using 0.1 M tetrabutylammonium hexafluorophosphate in anhydrous *N*,*N*-dimethylformamide as an electrolyte using a set of glassy carbon and two Pt wires as the working, counter, and reference electrodes, respectively. Ferrocene was used as an internal standard. A scan rate of 1000 mV s^{-1} has been applied. Before each measurement, samples were stirred for 15 s and left to equilibrate for 5 s.

X-ray crystal structure determination

The data collection for the crystal structures was measured at low temperature [100(2) K] using Mo Kα radiation on a Bruker APEX II CCD equipped with a kappa geometry goniometer. The data were reduced using EvalCCD[56] and then corrected for absorption.[57] The solutions and refinements were performed using SHELX.[58] The structures were refined using full-matrix least-squares based on F^2 with all non-hydrogen atoms anisotropically defined. Hydrogen atoms were placed in calculated positions by means of the "riding" model.

General method for the synthesis of 2,3′-bipyridine chloro-bridged dimer complexes

$[Ir(COD)(\mu\text{-}Cl)]_2$ (500 mg, 0.74 mmol) was suspended in 10 mL of 2-ethoxyethanol. The suspension was filled with nitrogen by 3 cycles vacuum/nitrogen. The ligand L (2.98 mmol, 4.0 equiv.) was added, and 1 mL of 2-ethoxyethanol was used for rinsing. The mixture was filled again with nitrogen by 3 cycles vacuum/nitrogen. The flask was sealed and heated at 130 °C. After 3 h, the mixture was cooled down. The volume of solvent was reduced to half under vacuum and 20 mL of methanol was added. The resulting precipitate was filtered, washed with methanol, and dried to afford the chloro-bridged iridium dimer $[Ir(L)_2(\mu\text{-}Cl)]_2$.

$[Ir(L5)_2(\mu\text{-}Cl)]_2$. L was 2′,6′-difluoro-2,3′-bipyridine (L5). The chloro-bridged iridium dimer $[Ir(L5)_2(\mu\text{-}Cl)]_2$ was obtained as a pale yellow solid (824 mg, 95%). ^1H NMR ($CDCl_3$, 400 MHz): δ 9.05 (broad d, 4H, J = 5.8 Hz); 8.36 (broad d, 4H, J = 8.2 Hz); 7.98 (broad dd, 4H, J = 7.9 Hz); 6.96 (broad dd, 4H, J = 6.4 Hz); 5.22 (s, 4H).

$[Ir(L6)_2(\mu\text{-}Cl)]_2$. L was 2′,6′-dimethoxy-2,3′-bipyridine (L6). The chloro-bridged iridium dimer $[Ir(L6)_2(\mu\text{-}Cl)]_2$ was obtained as a yellow solid (877 mg, 89%). ^1H NMR ($CDCl_3$, 400 MHz): δ 9.04 (broad d, 4H, J = 5.4 Hz); 8.47 (broad d, 4H, J = 8.2 Hz); 7.66 (broad ddd, 4H, J = 8.5, 1.2 Hz); 6.62 (broad dd, 4H, J = 6.1 Hz); 4.85 (s, 4H); 3.96 (s, 12H); 3.59 (s, 12H).

$[Ir(L7)_2(\mu\text{-}Cl)]_2$. L was 6′-methoxy-2′-methyl-2,3′-bipyridine (L7). The chloro-bridged iridium dimer $[Ir(L7)_2(\mu\text{-}Cl)]_2$ was obtained as a yellow solid (795 mg, 87%). ^1H NMR ($CDCl_3$, 400 MHz): δ 9.17 (broad d, 4H, J = 5.3 Hz); 8.01 (broad d, 4H, J = 8.3 Hz); 7.76 (broad ddd, 4H, J = 8.3 Hz); 6.73 (broad ddd, 4H, J = 5.3 Hz); 5.00 (s, 4H); 3.61 (s, 12H); 2.74 (s, 12H).

Synthesis of $[Ir(L7)_2(Pic)]$ EB343

2-Picolinic acid (98%, 98 mg, 2.00×10^{-4} mol, 4.0 eq.) and TBAOH (170 mg, 4.2 eq.) were dissolved in CH_2Cl_2–MeOH, 7/3 volume to volume, and this solution was added to a suspension of $[Ir(L7)_2(\mu\text{-}Cl)]_2$ (250 mg, 2.00×10^{-4} mol) CH_2Cl_2 (10 mL). The solution was gently refluxed at 40 °C under nitrogen overnight. After cooling down to room temperature, the solution was evaporated to dryness. The crude material was dissolved in pure CH_2Cl_2 and filtered over a pad of neutral silica. The volume of the solution was reduced under vacuum and the main fraction was slowly precipitated with hexane. The suspension was filtered off, washed with hexane, and dried under vacuum to afford **EB343** as a yellow solid (199 mg, 70%). ^1H NMR ($CDCl_3$, 400 MHz): δ 8.78 (broad ddd, 1H, J = 5.7, 1.5 Hz); 8.30 (broad d, 1H, J = 7.7 Hz); 8.01 (broad d, 1H, J = 8.5 Hz); 7.97 (broad d, 1H, J = 8.5 Hz); 7.89 (ddd, 1H, J = 7.7, 1.5 Hz); 8.72 (m, 3H); 7.45 (broad ddd, 1H, J = 5.7, 1.0 Hz); 7.35 (ddd, 1H, J = 5.4, 2.2, 1.5 Hz); 7.09 (ddd, 1H, J = 5.7, 1.3 Hz); 6.86 (ddd, 1H, J = 6.0, 1.3 Hz); 5.59 (s, 1H); 5.31 (s, 1H); 2.79 (s, 3H); 3.72 (s, 3H); 2.80 (s, 3H); 2.74 (s, 3H). ESI-TOF HRMS: MH^+ m/z: calc. 714.1694 found 714.1661. Anal. calcd for $C_{30}H_{26}IrN_5O_4$: C, 50.55; H, 3.68; N, 9.83. Found C, 50.45; H, 3.64; N, 9.86.

Results and discussion

Structure–property relationships based on Hammett parameters

The electrochemical gap ΔE_{REDOX} is usually well correlated with the emission maximum (optical gap) λ_{em}. However they are not strictly equivalent as the optical gap is smaller than the electrochemical gap.[59] The relation between ΔE_{PHOTO} and ΔE_{REDOX} is of the form:

$$\Delta E_{PHOTO} = \Delta E_{REDOX} + \sum_i \alpha_i \quad (1)$$

where the additional term collects factors not directly derivable from ΔE_{PHOTO} and ΔE_{REDOX}, such as Coulomb terms (electron repulsion, singlet/triplet states), solvation energy differences, and energy differences of relevant orbitals, for the four species involved: the complex in the ground state, the complex in the excited state, the oxidized complex, and the reduced complex. Nevertheless, within a same family of molecules, it is usually assumed that the difference between electrochemical and optical gaps is fairly constant, and eqn (2) can be used:

$$\Delta E_{PHOTO} \propto \Delta E_{REDOX} = E_{OX} - E_{RED} \quad (2)$$

When correlations between E_{OX} and σ are reported in the literature, the value of σ_m or σ_p is chosen based on the position of the substituent with respect to the carbon C coordinated to the iridium. This carbon atom is therefore a minimal representation of the HOMO of the complex. The oxidation potential of the corresponding complex is then expressed as a linear function of the Hammett parameters as follows:

$$E_{OX} = A\sigma_C + B \quad (3)$$

where σ_C is the sum of Hammett parameters with respect to C for all substituents on the ligand. As discussed in the Introduction, the substituents on the cyclometalated phenyl can impact the energy of the LUMO localized on the pyridine ring. Similarly, substituents on the pyridine are expected to impact the energy of the HOMO. However the impact will be attenuated due to the longer distance between the substituent on the pyridine ring and the carbon C, so that σ_C is rewritten as:

$$\sigma_C = \sum \sigma_{Phen_C} + \alpha \sum \sigma_{Pyr_C} \quad (4)$$

where σ_{Phen_C} are the Hammett parameter values with respect to C of the substituents on the phenyl, σ_{Pyr_C} are the Hammett parameter values with respect to C of the substituents on the pyridine, and α is the attenuation factor. Considering that $\sigma_p = \sigma_o$ and replacing according to the nomenclature introduced in Scheme 1, we can combine the relation with eqn (3) to obtain the general expression of E_{OX} as a function of the Hammett parameters of the substituents:

$$E_{OX} = A[(\sigma_{m_{R2}} + \sigma_{p_{R3}} + \sigma_{m_{R4}} + \sigma_{p_{R5}}) + \alpha(\sigma_{p_{R3'}} + \sigma_{m_{R4'}} + \sigma_{p_{R5'}} + \sigma_{m_{R6'}})] + B \quad (5)$$

Although no relation between reduction potentials E_{RED} and Hammett parameters has been reported before for cyclometalated iridium complexes, we can reasonably assume that such a relation exists using a similar approach to the oxidation potentials when the LUMO of the complex is mainly localized on the neutral ring of the orthometallated ligand. The nitrogen atom N (Scheme 1) is now considered as a reduced representation of the LUMO of the complex. The reduction potential of the corresponding complex is then expressed as a linear function of the Hammett parameters as follows:

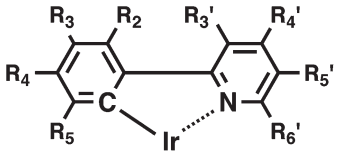

Scheme 1 Definition of the substitution pattern of the cyclometalated phenylpyridine ligand, as used in this work.

$$E_{RED} = C\sigma_N + D \quad (6)$$

where σ_N is the sum of Hammett parameters with respect to N for all substituents on the ligand. Developing the expression according to the nomenclature introduced in Scheme 1, we obtain the relation:

$$E_{RED} = C[(\sigma_{m_{R3'}} + \sigma_{p_{R4'}} + \sigma_{m_{R5'}} + \sigma_{p_{R6'}}) + \beta(\sigma_{p_{R2}} + \sigma_{m_{R3}} + \sigma_{p_{R4}} + \sigma_{m_{R5}})] + D \quad (7)$$

In order to develop a reliable predictive model, we focused on *fac*-tris-homoleptic cyclometalated iridium(III) complexes to avoid the interplay of ancillary ligands. It should be noted that no correlation is reported in the literature with substituents on the pyridine ring, as well as no correlation with reduction potentials. We used data from the literature[11,49,60] to obtain the values for A, B, C, D, α, and β from a multiple linear regression (Fig. 1). We did not take into account any solvent effect or differences in measurement conditions and we recalculated all potentials *vs.* ferrocene.[61,62] We also used the potentials of $[Ir(ppy)_3]$ as reported in ref. 11 as reference data

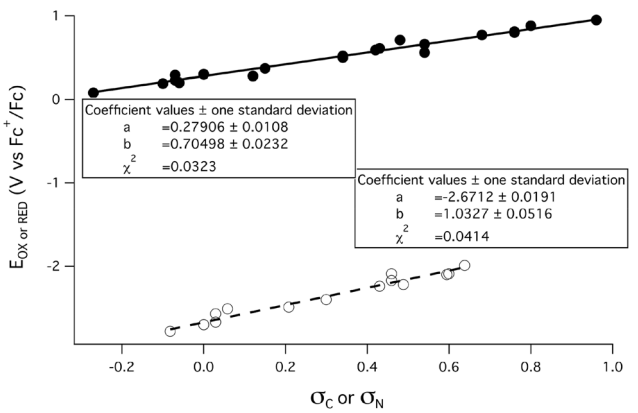

Fig. 1 Correlation between σ_C and E_{OX} (●) and σ_N and E_{RED} (○); the lines are of the form $a + bx$.

for other data sets. We obtained eqn (8) for E_{OX} in V *vs.* ferrocene, and eqn (9) for E_{RED} in V *vs.* ferrocene:[63]

$$E_{OX} \approx 0.7\left(\sum \sigma_{Phen_C} + 0.8\sum \sigma_{Pyr_C}\right) + 0.3 \quad (8)$$

$$E_{RED} \approx \left(\sum \sigma_{Pyr_N} + 0.5\sum \sigma_{Phen_N}\right) - 2.7 \quad (9)$$

Using eqn (2), we obtain the general relation for the redox gap ΔE_{REDOX} and the Hammett parameters σ in eqn (10):

$$\begin{aligned}\Delta E_{REDOX} \approx &\{0.7[(\sigma_{m_{R2}} + \sigma_{p_{R3}} + \sigma_{m_{R4}} + \sigma_{p_{R5}}) \\ &+ 0.8(\sigma_{p_{R3'}} + \sigma_{m_{R4'}} + \sigma_{p_{R5'}} + \sigma_{m_{R6'}})] + 0.3\} \\ &- \{[(\sigma_{m_{R3'}} + \sigma_{p_{R4'}} + \sigma_{m_{R5'}} + \sigma_{p_{R6'}}) \\ &+ 0.5(\sigma_{p_{R2}} + \sigma_{m_{R3}} + \sigma_{p_{R4}} + \sigma_{m_{R5}})] - 2.7\} \\ &= \sigma_{TOTAL} + 3\end{aligned} \quad (10)$$

For the parent complex [Ir(ppy)$_3$], all σ values are equal to 0 and the result is a $\Delta E_{REDOX} \approx 3$ eV.[11] Eqn (10) is the general quantitative relationship linking the electronic character of the substituents, as defined from their Hammett parameters, and the electrochemical gap of *fac*-tris-homoleptic iridium complexes based on 2-phenylpyridine cyclometalated ligand. The correlation between ΔE_{PHOTO}, that is, λ_{em}, and σ_{TOTAL} is shown in Fig. S2 (see ESI†). Although the values of A, B, C, D, α, and β are expected to vary with the ligand skeleton, and should be redefined in the case of cycles with a different number of atoms than six, the relation is qualitatively useful for other cyclometalated complexes (see below and ESI†).

With eqn (10) in hand, we now look at the effect of a single substituent, and its impact on the redox gap depending on its position, in particular to obtain blue-shifted emission compared to the parent complex [Ir(ppy)$_3$]. Within the same family of molecules, we assume that the difference between electrochemical and optical gaps is fairly constant. Using this simplification, the condition to obtain a blue shifted emission compared to [Ir(ppy)$_3$] is a larger redox gap:

$$\Delta E_{REDOX\ Blue} > \Delta E_{REDOX\ ppy} \quad (11)$$

For a substituent R_4, only σ_{mR4} and σ_{pR4} are non-zero. Using $\sigma_{mR4} = \sigma_m$ and $\sigma_{pR4} = \sigma_p$ in eqn (10), we obtain the simple relation:

$$\sigma_m - 0.7\sigma_p > 0 \quad (12)$$

A substituent fulfilling this condition will result in a larger redox gap than [Ir(ppy)$_3$] and thus in an expected blue shift of the emission. The first term, here σ_m, represents the influence of the substituent on the HOMO energy level and corresponds to the commonly used correlation between Hammett parameters and E_{OX}. The second term, here σ_p, represents the influence of the substituent on the LUMO energy level. This influence is less than unity, coefficient 0.7, which is well in line with the standard rule of thumb that substituents on the orthometallated phenyl influence more the HOMO than the LUMO.

Similarly, a substituent in position 3 needs to fulfill the condition in eqn (13) to result in a larger redox gap, and hence an expected blue shifted emission compared to [Ir(ppy)$_3$]:

$$\sigma_p - 0.7\sigma_m > 0 \quad (13)$$

In the same way as for the substituents on the phenyl, simple relations can be derived for substituents on the pyridine. For a substituent on position 5′:

$$\sigma_m - 0.5\sigma_p < 0 \quad (14)$$

and for a substituent on position 4′:

$$\sigma_p - 0.5\sigma_m < 0 \quad (15)$$

Compared to the case of substituents on the phenyl, the first term here represents the impact of the substituent on the LUMO energy level, while the second term is the impact on the HOMO energy level. It is interesting to note that for substituents on the pyridine, the effect on the remote orbital, the HOMO, is smaller than the effect on the LUMO of a substituent on the phenyl (coefficient 0.5 compared to 0.7).

These attenuation values can be compared to the extent of delocalization of the HOMO and LUMO over the entire C^N ligand obtained from DFT(M06)/IEF-PCM(ACN) calculations. The extent of HOMO on the pyridine is much smaller than the one of LUMO on the orthometallated phenyl (Fig. 2). While 33% of the HOMO is localized on the orthometallated phenyl of [Ir(ppy)$_3$], only 7% is found on the pyridine (the remaining contribution is found on the iridium). This proportion is reversed for the LUMO of [Ir(ppy)$_3$], where now 60% is localized on the pyridine, while as much as 38% lies on the phenyl ring. Therefore it is not surprising that the impact on the HOMO energy level of a substituent on the pyridine will be smaller than the impact on the LUMO energy level of a substituent on the phenyl. It is very satisfying that our simple and naïve model can qualitatively reproduce such results from advanced theoretical calculations.

Using eqn (12) and (13) to calculate the conditions on the Hammett parameters in the series of complexes reported by Watts and coworkers,[49] the observed emissions are now as

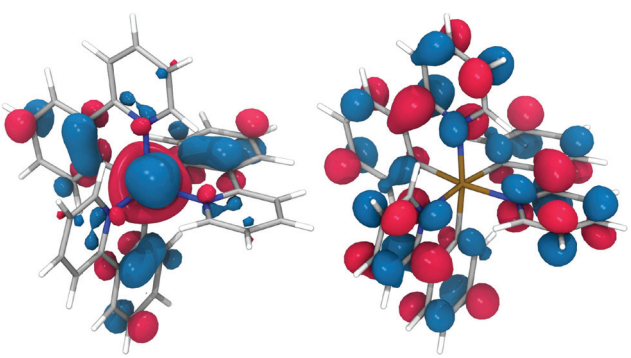

Fig. 2 Kohn–Sham HOMO (left) and LUMO (right) of the *fac*-tris homoleptic compound [Ir(ppy)$_3$], obtained at the DFT(M06)/IEF-PCM(ACN) level of theory.

expected (Table 1). In particular the effect of the $-CF_3$ group on position 4 is now understood in a very simple manner: due to its high σ_p value, this substituent influences the LUMO as much as the HOMO and the resulting HOMO–LUMO gap is the same as for [Ir(ppy)$_3$] (condition = 0.05, λ_{em}[Ir(4-CF_3-ppy)$_3$] $\approx \lambda_{em}$[Ir(ppy)$_3$]). The methoxy case is also explained for the case when on position 4 the condition is positive (blue shift) and on position 5 the condition is negative (red shift). It should be stressed that the model calculates the redox gap and not the emission gap ΔE_{PHOTO}, which explains the similar value of the condition for the methoxy group on position 4 compared to fluoride, despite the fact that fluoride substituted compounds show a more pronounced blue-shift of the emission (see below).

To evaluate the applicability of the relations derived for *fac*-tris-homoleptic iridium(III) complexes to other systems based on cyclometalated 2-phenylpyridine ligands, we applied them to a series of [Ir(R-ppy)$_2$(acac)],[9,55,64–67] [Ir(R-ppy)$_2$(pic)],[54,68–70] and [Pt(R-ppy)(acac)][71,72] complexes, with acac = acetylacetonate, pic = picolinate, and R-ppy = substituted 2-phenylpyridine. The results are shown in ESI (Fig. S3–S5†). The numeric values obtained from [Ir(R-ppy)$_3$] have been directly used in eqn (4), (6), and (10) without new calculations. It is therefore remarkable that the oxidation potentials are still well correlated with σ_C in the cases of [Ir(R-ppy)$_2$(acac)] and [Ir(R-ppy)$_2$(pic)] complexes. However, correlations between ΔE_{REDOX} and λ_{em} are much less satisfactory. Besides the various measurement conditions, in particular the solvent,[73] and the difference between ΔE_{REDOX} and ΔE_{PHOTO} (see eqn (1)), substituents possibly resulting in extended aromatic ligand systems, such as carboxylic acid, ester, acetyl, and dimethylamino groups, are more red shifted than anticipated by the model based on redox potentials. In the case of [Pt(R-ppy)(acac)], the correlation between ΔE_{REDOX} and λ_{em} is now remarkable, while the correlation between the reduction potentials and σ_N is less satisfactory. λ_{em} for both data sets used the same solvent at 77 K, in contrast to various solvents at room temperature for the [Ir(R-ppy)$_2$(acac)] and [Ir(R-ppy)$_2$(pic)] series, which may explain the apparent improved correlation.

The model will fail when the HOMO and LUMO are not localized on, respectively, the phenyl and pyridine of the main ligand. For example, when a chromophoric ancillary ligand such as 2,2′-bipyridine is used, correlation would be found only between E_{OX} and σ_C because the LUMO is localized on the ancillary ligand. A similar failure of the model was observed when the frontier orbitals are localized on a substituent instead of the main ligand.[68]

We presented here a very simple relationship between Hammett parameters and electrochemical properties of cyclometalated iridium complexes. In particular, eqn (12)–(15) are straightforward to apply and give a reliable condition on the substituents to tune the redox potentials and the emission wavelength. Due to the small data set used to derive the numerical values and the approximations made concerning the experimental measurement conditions, the relations are reasonably quantitative for tris-cyclometalated ppy-based complexes and quasi-quantitative to qualitative in other cases. These relations clearly explain the unusual position effect of substituents such as $-CF_3$ and –OMe. This result quantitatively demonstrates that a strong acceptor will not necessarily result in blue-shifted emission, and that electron-donating groups can be used on the orthometallated phenyl to obtain a blue shift of the emission.

Donor groups on orthometallated phenyl for a blue shift of emission

The most common strategy to blue shift the emission of cyclometalated iridium complexes is to use acceptor substituents on the orthometallated phenyl ring, often using fluorine substituents on positions 2 and 4. However, those complexes are particularly unstable in electroluminescent devices. In addition to the high energy content of the blue exciton resulting in a thermally accessible antibonding metal-centered state,[74] the strong electron-withdrawing character of fluorine leads to chemical degradation in operational devices.[75–77] The possibility to replace the acceptor fluorine with a donor group in blue phosphorescent emitters is therefore particularly attractive. To further explore the effect of electron-donating groups on the emission maximum of iridium complexes and to exploit the possibility of replacing fluorine acceptor substituents by methoxy donor groups for blue emission, we prepared a series of novel complexes (Scheme 2) and compared them with known emitters, namely [Ir(ppy)$_2$(acac)] (**1**), [Ir(diFppy)$_2$(acac)] (**2**), and **FIrPic**.

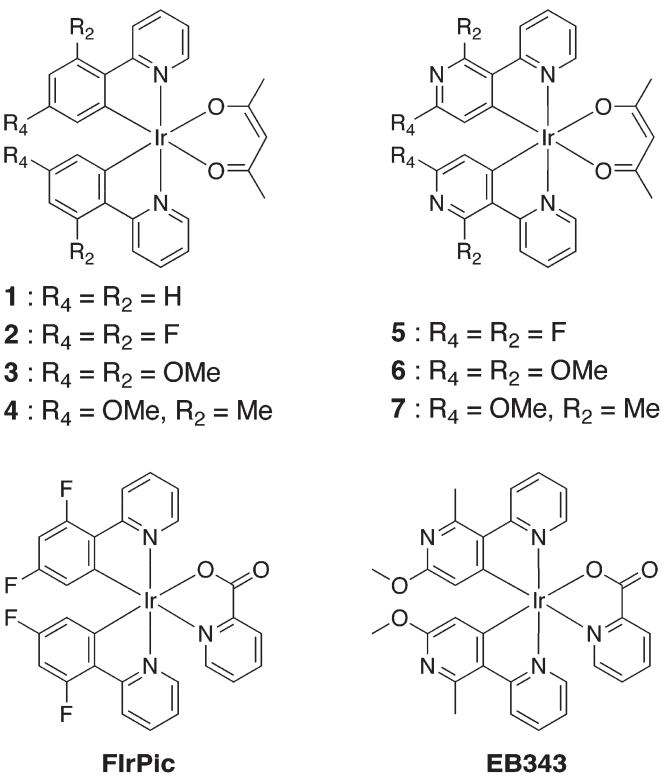

Scheme 2 Chemical structure of the complexes studied in this work.

To effectively replace electron-withdrawing fluorine, in addition to maintaining identical emission maximum it is also preferable to have identical molecular orbital energy levels. In this case, the architecture of the whole electroluminescent device could be kept identical, simply replacing fluorine-based emitters with donor-based emitters. To tune the oxidation and reduction of donor-substituted complexes towards higher potentials, we introduced a nitrogen atom in place of the R_3-substituent of the cyclometalating ligand. This modification produces a negative shift of both HOMO and LUMO.[78–80] Combining the donor-substituents with 2,3′-bipyridine we developed complexes with similar electrochemical and emission properties as complexes based on 2,4-difluorophenylpyridine.

Synthesis

The ligands used in this study were prepared by conventional Suzuki coupling. It is important to stress that very clean ligands, which are indispensable for the isolation of pure iridium dimers, could only be obtained after several chromatography purifications (see the Experimental part for details). Dimer precursors to complexes **1–4** were prepared according to the report of Watts and coworkers.[81] Stoichiometric amounts of the cyclometalating ligand and $IrCl_3$ were refluxed overnight at 130 °C in a mixture of 2-ethoxyethanol–water. Unfortunately, these standard conditions proved inefficient when 2,3′-bipyridine ligands were used, and the corresponding dimers could be isolated in low yields only (for example with the dimer-precursor of **3**, isolated yield is 6%). Although we do lack clear evidence regarding the side-products that are formed during the reaction, we suspect that protons released in solution, as a result of cyclometalation, induce cleavage of the methoxy groups of the ligands. This prompted us to explore an alternative source of iridium in order to avoid such degradation.

Encouraged by the recent success we experienced using $[Ir(COD)(\mu\text{-}Cl)]_2$ for the synthesis of tris-heteroleptic complexes,[55,82] we tested similar conditions to prepare the 2,3′-bipyridine-based dimers. Contrary to $IrCl_3$ that cyclometalates *via* electrophilic aromatic substitution, COD-precursors of iridium usually proceed initially by oxidative addition owing to the low oxidation degree of the metal.[83] This particular reactivity is well exploited in catalytic C–H bond activations where very active and selective complexes are needed.[84] Gratifyingly, when stoichiometric amounts of 2′,6′-dimethoxy-2,3′-bipyridine or 6′-methoxy-2′-methyl-2,3′-bipyridine are reacted with $[Ir(COD)(\mu\text{-}Cl)]_2$ in 2-ethoxyethanol at 130 °C, very clean dimers are obtained quickly (usually in about 3 hours) and in good yields (see ESI†). With the various dimers in hand, both acac and pic complexes become readily accessible following a standard procedure. By gently refluxing the chloro-bridged complex with acetylacetone or picolinic acid in the presence of a base, the final compounds could be isolated in good yields by simple filtration over neutral silica to avoid cleavage of the ancillary ligand[55] followed by recrystallization from a dichloromethane–methanol or dichloromethane–hexane mixture. Full experimental details and characterizations (^1H and ^{19}F NMR, elemental analysis and high-resolution mass spectrometry) are available in ESI.†

X-ray single crystal structures

Single crystals of **1–4**, **6**, and **7** were obtained by slow diffusion of hexane or methanol in a dichloromethane solution of the complex. Structures are shown in Fig. 3 and selected bond lengths and angles are given in Table 2. Crystallographic parameters are given in Table S2.† As expected, all complexes adopt a distorted octahedral geometry around the iridium center with N-binding pyridines in *trans* positions relative to each other. Overall the geometry around the metal is not significantly influenced by the ligand used. Whether the latter is phenylpyridine or 2,3′-bipyridine, similar bond lengths and angles are observed throughout the series. Similarly, there is no net variation in the Ir–O bond length between the iridium center and the acetylacetonate ancillary ligand. However, the main ligand is markedly impacted by the R_2 and R_4 substituents at the cyclometalating ring. Firstly, modification of the substitution pattern translates into an elongation of the C_1–C_2' bond that links both rings of the cyclometalating ligand as evidenced by comparing complexes **2–4** and **6–7** with **1**. Secondly, torsions of up to 6.0° are observed for the C_3'–C_2'–C_1–C_2 angle when methyl and methoxy substituents are used, in contrast to complexes **1** and **2**. This is particularly evident for complexes **4** and **7** where a methyl group is introduced at the R_2-position. This deformation is also accompanied by a severe torsion between the R_2-group and the plane of the cyclometalating ligand (C_2'–C_1–C_2–R_2 angle) as observed for complexes **3–4** and **6–7** in contrast to **1** and **2**. Finally, R_2 and R_4 substituents tend to deviate from the plane of the cyclometalating ring, as exemplified by the R_2–C_2–X–C_4 and C_2–X–C_4–R_4 torsion angles, with a more pronounced effect when methyl groups are used.

Electrochemical properties

The electrochemical properties of the complexes were recorded in dimethylformamide. Data are summarized in Table 3. As expected, each complex shows quasi-reversible to irreversible one-electron processes in both positive and negative bias (see Fig. S6†). The anodic peak potential is ascribed to oxidation of the iridium(III) metal center to iridium(IV) while the two cathodic peaks are assigned to reduction of the phenylpyridine or 2,3′-bipyridine ligands depending on the complex.[32] For **EB343** and **FIrPic**, an additional third reduction is observed within the range of potential scan; they are attributed to the reduction of the picolinate ligand (Fig. 4).

As evidenced by comparing the electrochemical data of **3** and **4** with reference complex **1**, decorating the phenyl ring with methoxy and methyl groups increases the electrochemical gap. A similar effect is seen for **2** when electron-withdrawing fluorine groups are used. Nevertheless, in contrast to fluorines that induce a greater stabilization of the HOMO than the LUMO due to the large positive value of σ_m, the combination of methoxy and methyl substituents operates by destabilizing the LUMO more than the HOMO due to the large negative value of σ_p, as expected from the Hammett parameter-based

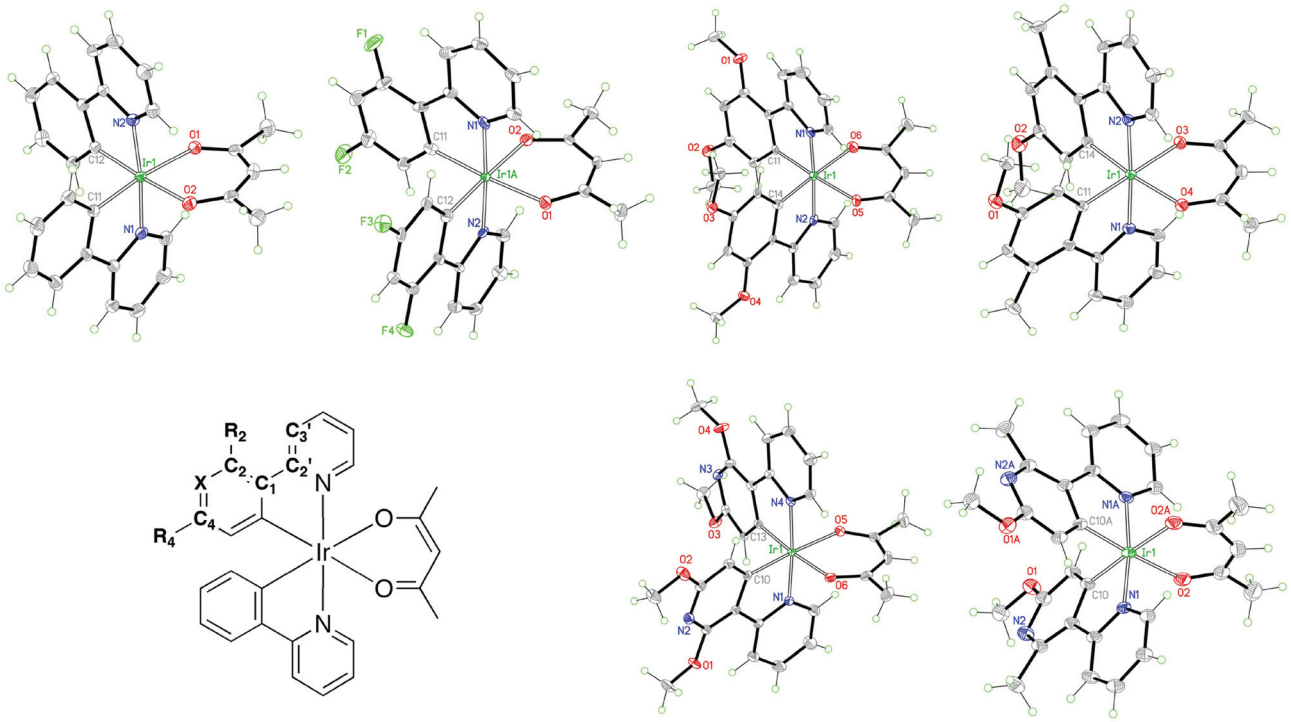

Fig. 3 ORTEP drawings from left to right of (top) **1**, **2**, **3**, **4** and (bottom) **6** and **7**. The labels for selected atoms as used in Table 2 are shown on the general structure of the complexes.

Table 2 Average of selected bond lengths (Å) and angles (°) for complexes **1**, **2**, **3**, **4**, **6** and **7**

Bond lengths	1	2	3	4	6	7
Ir–N	2.037	2.042	2.039	2.036	2.037	2.042
Ir–C	1.992	1.995	1.985	1.990	1.983	1.981
Ir–O	2.159	2.147	2.153	2.160	2.147	2.156
C_1–C_2'	1.458	1.466	1.465	1.473	1.460	1.473
Bond angles						
N–Ir–N	173.86	176.37	176.85	175.93	177.26	173.11
C–Ir–C	90.82	88.67	90.60	88.00	90.86	89.19
C–Ir–O	91.25	91.42	90.57	92.31	90.55	91.36
O–Ir–O	87.27	88.95	88.47	87.66	88.33	88.45
Torsion angles						
C_3'–C_2'–C_1–C_2	2.03	0.90	4.39	4.78	1.79	6.02
C_2'–C_1–C_2–R_2	—	1.30	5.40	2.84	4.06	12.76
R_2–C_2–X–C_4	—	179.67	179.21	177.45	177.72	175.83
C_2–X–C_4–R_4	—	178.52	179.27	179.40	178.74	176.48

Table 3 Oxidation and reduction potentials, electrochemical gap of complexes **1–7**, **FIrPic**, and **EB343** in dimethylformamide (0.1 M $TBAPF_6$). Potentials are listed in V *vs.* the Fc^+/Fc couple. The peak-to-peak separations between the anodic and the cathodic peak potentials ($\Delta E = E_{pa} - E_{pc}$) are indicated in parentheses in mV

	E_{OX}	E_{RED}	ΔE_{REDOX}	σ_{TOTAL}
1	0.41 (95)	−2.60 (125)	3.01	0
2	0.76 (115)	−2.44 (115)	3.20	0.60
3	0.42 (145)	−2.77 (–), −3.29 (–)	3.19	0.62
4	0.35 (225)	−2.72 (145)	3.07	0.36
5	1.08 (–)	−2.29 (145), −2.57 (225)	3.37	
6	0.74 (155)	−2.69 (–)	3.43	
7	0.74 (145)	−2.59 (145), −2.88 (–)	3.33	
EB343	0.93 (165)	−2.32 (185), −2.76 (180), −3.08 (200)	3.26	
FIrPic	0.93 (150)	−2.28 (150), −2.62 (170), −2.98 (200)	3.21	

structure–property relationships discussed above. Electron-donating groups can therefore produce the desired blue-shift in emission (see photophysical properties).

Introducing a nitrogen atom in place of the R_3-substituent of the cyclometalating ligand produces a negative shift of both HOMO and LUMO as shown by the apparent electrochemical potentials measured for complexes **5**–**7**. More specifically, changing the HOMO-localized ring from phenyl to pyridine shifts the oxidation potential positively by *ca.* 300 mV (the difference measured between complexes **4** and **7** is attributed to the poor reversibility of the oxidation of **7**). This observation is in line with previous reports where 2′,6′-difluoro-2,3′-bipyridine was used to obtain deep-blue emissions.[78–80] As expected, modification of the substitution pattern impacts the LUMO levels of the complexes as well, because of the electronic communication between both cyclometalating and N-coordinating pyridines. This is manifest on the first reduction potentials of **5**, **6** and **7**, which are lowered by *ca.* 100–150 mV compared to **2**, **3** and **4**, respectively.

By comparing the electrochemical properties of **2** with **7**, one can realize that the 6′-methoxy-2′-methyl-2,3′-bipyridine ligand is quasi-isoelectronic to a 2,4-difluorophenylpyridine. As a result, the main ligand used in **FIrPic** can now be replaced while retaining the properties of the complex. This is strikingly

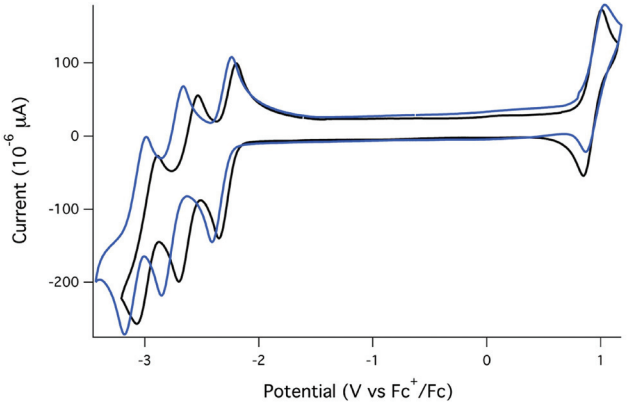

Fig. 4 Cyclic voltammogram comparison between **EB343** (—) and **FIrPic** (—) recorded in dimethylformamide at a scan rate of 1000 mV s^{-1}.

evident from the electrochemistry of **EB343**. The new fluorine-free complex displays oxidation and reduction potentials that are virtually identical to that of the standard sky-blue emitting **FIrPic** complex (Fig. 4).

UV-visible absorption spectra

The UV-visible absorption spectra of all complexes were measured in solution in acetonitrile (Fig. 5 and Table 4). All spectra display a similar overall profile and, by analogy with previously reported assignations, the intense absorption bands in the UV region ($\lambda_{abs} \approx 250$–$300$ nm and $\varepsilon \approx 40 \times 10^3$ M^{-1} cm^{-1}) are attributed to ligand centered (LC) $^1(\pi$–$\pi^*)$ transitions,[9] while the weaker and lower-energy absorption bands correspond to metal-to-ligand charge transfer (^{1}MLCT) transitions.[85] Finally, the lowest energy transitions with $\varepsilon < 10^3$ M^{-1} cm^{-1} are ^{3}MLCT transitions caused by direct population of the emitting triplet state.[54] Compared to the model complex **1**, the presence of substituents has practically no influence on the intensity of the LC and ^{3}MLCT bands. In contrast, the methoxy groups have a significant impact on the intensity of the ^{1}MLCT bands, which more than doubles upon addition of two methoxy groups (at $\lambda_{abs} = 335$ nm: $\varepsilon \approx 9 \times 10^3$ M^{-1} cm^{-1} for **1** and **2**; $\varepsilon \approx 15 \times 10^3$ M^{-1} cm^{-1} for **4** with one –OMe group; $\varepsilon \approx 22 \times 10^3$ M^{-1} cm^{-1} for **3** with two –OMe groups).

As expected from the Hammett parameter-based model discussed above, the onset of absorption (defined as $\varepsilon = 100$ M^{-1} cm^{-1}) is blue-shifted as methoxy groups are added to the main ligand. However, in contrast to the electrochemical gaps which are identical for **2** and **3**, as anticipated by the values of σ_{TOTAL}, the onset of absorption of **2** is 13 nm (~600 cm^{-1}) blue-shifted compared to **3**. This means that the additional term $\sum a_i$ relating ΔE_{PHOTO} and ΔE_{REDOX} in eqn (1) is not constant on going from **2** to **3**, although in both cases the skeleton of the main ligand is phenylpyridine.

The replacement of the 2-phenylpyridine core with 2,3′-bipyridine simply leads to 20–25 nm (~1000 cm^{-1}) blue shift of the onset of absorption without significant other changes in the absorption spectra.

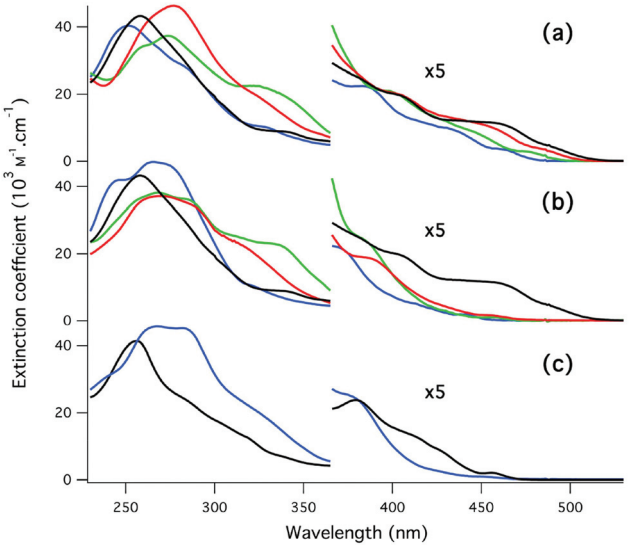

Fig. 5 UV-visible absorption spectra of complexes in acetonitrile: (a) **1** (—), **2** (—), **3** (—), **4** (—); (b) **1** (—), **5** (—), **6** (—), **7** (—); (c) **FIrPic** (—), **EB343** (—).

Table 4 Data for complexes **1**–**7**, **EB343**, and **FIrPic**

	λ_{abs} (nm) (ε (10^3 L mol^{-1} cm^{-1}))[a]	λ_{em} [a] (nm) RT	λ_{em} [b] (nm) 77 K
1	258 (43.2), 342 (8.6), 398 (4.0), 456 (2.3), 487 (0.9)	528	506
2	252 (40.3), 328 (10.2), 383 (4.5), 428 (2.0), 458 (0.7)	491	472
3	260 (34.2), 274 (37.3), 326 (22.2), 398 (4.2), 473 (0.6)	500	486
4	277 (46.3), 320 (20.7), 358 (8.24), 401 (4.1), 484 (0.7)	519	495
5	246 (41.8), 265 (47.3), 370 (4.4), 439 (0.4)	(465) 480	447
6	268 (38.1), 333 (22.9), 384 (4.8), 457 (0.2)	470	461
7	270 (37.1), 286 (34.8), 322 (20.2), 388 (3.7), 456 (0.3)	(484) 497	464
EB343	268 (45.6), 281 (45.1), 320 (21.4), 380 (4.8), 449 (0.2)	(466) 492	456
FIrPic	253 (40.9), 282 (24.5), 316 (11.9), 375 (4.8), 455 (0.4)	469	458

[a] In acetonitrile. [b] In 2-methyltetrahydrofuran.

Luminescence spectra

With the exception of **6**, when excited at 298 K within the ligand (π–π^*) and MLCT absorption bands, the complexes show broad and poorly structured emissions that are characteristic of complexes containing a combination of cyclometalated ligands with acetylacetonate as the ancillary ligand (Fig. 6). At 77 K in 2-methyltetrahydrofuran (2-MeTHF), the spectra become highly structured and clear vibronic progressions are seen for all complexes (Fig. 7). Similar to the absorption spectra, the emission is blue-shifted as methoxy groups are added to the main ligand, 519 nm for **4** and 500 nm for **3** compared to 528 nm for reference **1** at room temperature, but not

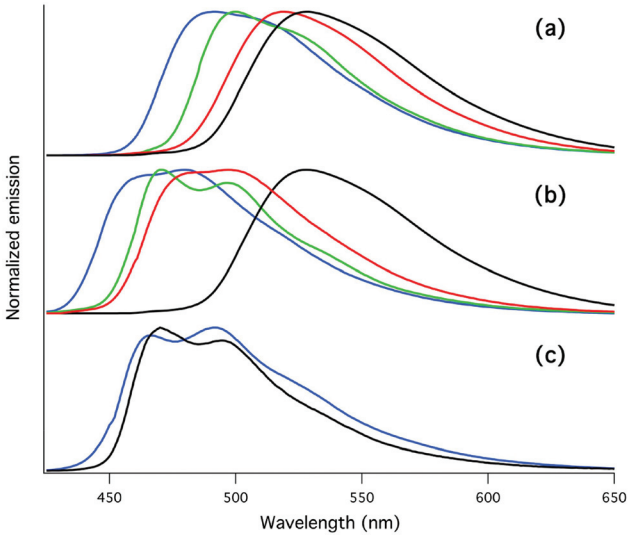

Fig. 6 Emission spectra of complexes in degassed acetonitrile at room temperature: (a) **1** (—), **2** (—), **3** (—), **4** (—); (b) **1** (—), **5** (—), **6** (—), **7** (—); (c) **FIrPic** (—), **EB343** (—).

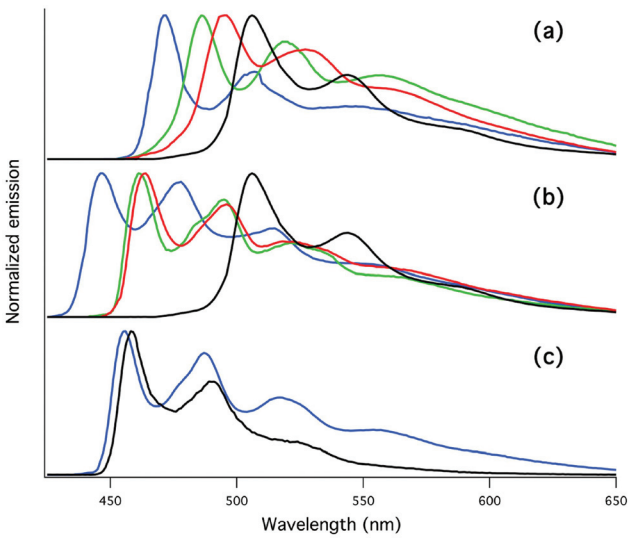

Fig. 7 Emission spectra of complexes in 2-methyltetrahydrofuran at 77 K: (a) **1** (—), **2** (—), **3** (—), **4** (—); (b) **1** (—), **5** (—), **6** (—), **7** (—); (c) **FIrPic** (—), **EB343** (—).

as much as with fluorine substituents, 491 nm, in contrast to the electrochemical gaps which are identical for **2** and **3**. This means that, as for the absorption, the additional term $\sum a_i$ relating $\Delta E_{\mathrm{PHOTO}}$ and $\Delta E_{\mathrm{REDOX}}$ in eqn (1) is not constant on going from **2** to **3**.

As for their electrochemical properties, **2** and **7** have also a very similar emission spectrum. As a result, the main ligand used in **FIrPic** can be replaced by the 6′-methoxy-2′-methyl-2,3′-bipyridine ligand in **EB343**. The emission spectra of **EB343** compared to **FIrPic** are shown in Fig. 6c at room temperature and Fig. 7c at 77 K. The new fluorine-free complex displays only a slightly blue shifted and broader emission compared to the standard sky-blue emitting **FIrPic** complex. The adiabatic E_{0-0} transition energies computed at the (U)DFT/M05-2X/IEF-PCM(ACN) level for **EB343** and **FIrPic** are close, 3.03 eV *vs.* 3.14 eV, respectively. In both cases, the emission exhibits a LC-MLCT character (see ESI†). The photoluminescence quantum yield and lifetime of the excited state of **EB343** and **FIrPic** in solution in degassed acetonitrile at room temperature are Φ = 0.54 and 0.61 and τ = 1.29 and 1.69 μs, respectively. Finally, to explore further the colours of emission offered by this new fluorine-free ligand, we used the chloro-bridged iridium dimer $[\mathrm{Ir(L7)_2(\mu\text{-}Cl)}]_2$ to screen ancillary ligands (Fig. S12†).[86]

Conclusions

We have described a simple quantitative model based on Hammett parameters that rationalizes the effect of the substituents on the properties of cyclometalated iridium(III) complexes. This model allows predicting the apparent redox potentials as well as the electrochemical gap of homoleptic complexes based on phenylpyridine ligands with good accuracy. Importantly, the model accounts for the unequal effect of the substituents on both the HOMO and the LUMO energy levels by taking into account both the σ_m and σ_p values of the Hammett constant for a given substituent. Consequently, the model can also be used to anticipate the emission maxima of the corresponding complexes with improved reliability. In particular, it was possible to rationalize in a very simple manner the influence on emission maxima of trifluoromethyl and methoxy groups and to demonstrate that a strong acceptor will not necessarily result in a blue-shifted emission, while electron-donating groups can be used on the orthometallated phenyl to obtain a blue-shift of the emission.

The main strength of this model is the simplicity of the approach and of the relations developed from it, which makes its application to a range of complexes based on cyclometalated 2-phenylpyridine straightforward. Further numeric improvements could be obtained by increasing the size of the database and having measurements performed under identical conditions. Conceptual improvements are expected by separating inductive and mesomeric effects and by distinguishing between *para* and *ortho* positions, especially due to the possible impact of steric hindrance of substituents on the properties of the complexes.[87] These improvements could result in a reliable relationship between Hammett constants and emission wavelength maxima. Finally, generalization beyond ppy could be obtained by combining the model in this work with concepts such as the ligand electrochemical parameter.[88,89]

In this work, we used this model to develop a series of emitters where electron-donating groups, methyl and methoxy, can effectively replace electron-withdrawing fluorine substituents on the orthometallated phenyl to induce a blue shift of the emission. This result is in contrast with the common approach that relies almost exclusively on fluorine to blue shift the emission maximum of a given complex. The blue shift induced by

fluorine is mainly due to the strong acceptor character towards the *meta* position, resulting in a stronger stabilization of the HOMO than the LUMO, while the blue shift induced by methoxy is mainly due to the strong donor character towards the *para* position, resulting in a stronger destabilization of the LUMO than the HOMO. The work also shows that the assumption that the difference between electrochemical and optical gaps is fairly constant within the same family of molecules should be used with caution.

Finally, as a proof of concept, we used a 2,3′-bipyridine as the skeleton of the main ligand with donor substituents and were able to match the various properties, namely oxidation and reduction potentials, electrochemical gap and emission profile, of the standard sky-blue emitter **FIrPic** with a new fluorine-free complex referred to as **EB343**.

Acknowledgements

We acknowledge financial support for this work by Solvay S.A. and the European Union (HetIridium, CIG 322280).

Notes and references

1 C. Alexiou and A. B. P. Lever, *Coord. Chem. Rev.*, 2001, **216–217**, 45.
2 J. K. Hino, L. Della Ciana, W. J. Dressick and B. P. Sullivan, *Inorg. Chem.*, 1992, **31**, 1072.
3 M. Lanznaster, A. Neves, A. J. Bortoluzzi, A. M. Assumpcao, I. Vencato, S. P. Machado and S. M. Drechsel, *Inorg. Chem.*, 2006, **45**, 1005.
4 C. Makedonas and C. A. Mitsopoulou, *Eur. J. Inorg. Chem.*, 2007, 4176.
5 B. H. Solis and S. Hammes-Schiffer, *J. Am. Chem. Soc.*, 2011, **133**, 19036.
6 A. R. Dick, J. W. Kampf and M. S. Sanford, *J. Am. Chem. Soc.*, 2005, **127**, 12790.
7 L. Flamigni, A. Barbieri, C. Sabatini, B. Ventura and F. Barigelletti, *Top. Curr. Chem.*, 2007, **281**, 143.
8 K. A. King, P. J. Spellane and R. J. Watts, *J. Am. Chem. Soc.*, 1985, **107**, 1431.
9 S. Lamansky, P. Djurovich, D. Murphy, F. Abdel-Razzaq, R. Kwong, I. Tsyba, M. Bortz, B. Mui, R. Bau and M. E. Thompson, *Inorg. Chem.*, 2001, **40**, 1704.
10 M. S. Lowry and S. Bernhard, *Chem.–Eur. J.*, 2006, **12**, 7970.
11 A. B. Tamayo, B. D. Alleyne, P. I. Djurovich, S. Lamansky, I. Tsyba, N. N. Ho, R. Bau and M. E. Thompson, *J. Am. Chem. Soc.*, 2003, **125**, 7377.
12 Y. You and S. Y. Park, *Dalton Trans.*, 2009, 1267.
13 E. Baranoff, J. H. Yum, M. Graetzel and M. K. Nazeeruddin, *J. Organomet. Chem.*, 2009, **694**, 2661.
14 M. A. Baldo, M. E. Thompson and S. R. Forrest, *Nature*, 2000, **403**, 750.
15 S. Bettington, M. Tavasli, M. R. Bryce, A. S. Batsanov, A. L. Thompson, H. A. Al Attar, F. B. Dias and A. P. Monkman, *J. Mater. Chem.*, 2006, **16**, 1046.
16 C. Adachi, M. A. Baldo, M. E. Thompson and S. R. Forrest, *J. Appl. Phys.*, 2001, **90**, 5048.
17 R. N. Bera, N. Cumpstey, P. L. Burn and I. D. W. Samuel, *Adv. Funct. Mater.*, 2007, **17**, 1149.
18 P. T. Chou and Y. Chi, *Chem.–Eur. J.*, 2007, **13**, 380.
19 S. Lamansky, P. Djurovich, D. Murphy, F. Abdel-Razzaq, H. E. Lee, C. Adachi, P. E. Burrows, S. R. Forrest and M. E. Thompson, *J. Am. Chem. Soc.*, 2001, **123**, 4304.
20 E. Orselli, G. S. Kottas, A. E. Konradsson, P. Coppo, R. Fröhlich, L. De Cola, A. van Dijken, M. Buchel and H. Börner, *Inorg. Chem.*, 2007, **46**, 11082.
21 J. A. G. Williams, A. J. Wilkinson and V. L. Whittle, *Dalton Trans.*, 2008, 2081.
22 J.-H. jou, M.-F. Hsu, W.-B. Wang, C.-L. Chin, Y.-C. Chung, C.-T. Chen, J.-J. Shyue, S.-M. Shen, M.-H. Wu, W.-C. Chang, C.-P. Liu, S.-Z. Chen and H.-Y. Chen, *Chem. Mater.*, 2009, **21**, 2565.
23 K. K. Lo, A. W. Choi and W. H. Law, *Dalton Trans.*, 2012, **41**, 6021.
24 H. J. Bolink, H. Brine, E. Coronado and M. Sessolo, *Adv. Mater.*, 2010, **22**, 2198.
25 R. D. Costa, E. Orti, H. J. Bolink, S. Graber, S. Schaffner, M. Neuburger, C. E. Housecroft and E. C. Constable, *Adv. Funct. Mater.*, 2009, **19**, 3456.
26 J. D. Nguyen, J. W. Tucker, M. D. Konieczynska and C. R. J. Stephenson, *J. Am. Chem. Soc.*, 2011, 1.
27 A. Valore, E. Cariati, C. Dragonetti, S. Righetto, D. Roberto, R. Ugo, F. De Angelis, S. Fantacci, A. Sgamellotti, A. Macchioni and D. Zuccaccia, *Chem.–Eur. J.*, 2010, **16**, 4814.
28 J. Sun, W. Wu and J. Zhao, *Chem.–Eur. J.*, 2012, **18**, 8100.
29 B. Happ, A. Winter, M. D. Hager and U. S. Schubert, *Chem. Soc. Rev.*, 2012, **41**, 2222.
30 C. Ulbricht, B. Beyer, C. Friebe, A. Winter and U. S. Schubert, *Adv. Mater.*, 2009, **21**, 4418.
31 L. Sun, A. Galan, S. Ladouceur, J. D. Slinker and E. Zysman-Colman, *J. Mater. Chem.*, 2011, **21**, 18083.
32 P. J. Hay, *J. Phys. Chem. A*, 2002, **106**, 1634.
33 T. Sajoto, P. I. Djurovich, A. Tamayo, M. Yousufuddin, R. Bau, M. E. Thompson, R. J. Holmes and S. R. Forrest, *Inorg. Chem.*, 2005, **44**, 7992.
34 A. Tsuboyama, H. Iwawaki, M. Furugori, T. Mukaide, J. Kamatani, S. Igawa, T. Moriyama, S. Miura, T. Takiguchi, S. Okada, M. Hoshino and K. Ueno, *J. Am. Chem. Soc.*, 2003, **125**, 12971.
35 Y. S. Yeh, Y. M. Cheng, P. T. Chou, G. H. Lee, C. H. Yang, Y. Chi, C. F. Shu and C. H. Wang, *ChemPhysChem*, 2006, **7**, 2294.
36 S. Bettington, M. Tavasli, M. R. Bryce, A. Beeby, H. Al-Attar and A. P. Monkman, *Chem.–Eur. J.*, 2007, **13**, 1423.
37 Z. Q. Gao, B. X. Mi, H. L. Tam, K. W. Cheah, C. H. Chen, M. S. Wong, S. T. Lee and C. S. Lee, *Adv. Mater.*, 2008, **20**, 774.

38 R. Wang, D. Liu, H. Ren, T. Zhang, X. Wang and J. Li, *J. Mater. Chem.*, 2011, **21**, 15494.
39 E. Baranoff, S. Fantacci, F. De Angelis, X. Zhang, R. Scopelliti, M. Grätzel and M. K. Nazeeruddin, *Inorg. Chem.*, 2011, **50**, 451.
40 G. Treboux, J. Mizukami, M. Yabe and S. Nakamura, *J. Photopolym. Sci. Technol.*, 2008, **21**, 347.
41 C. Hansch, A. Leo and R. W. Taft, *Chem. Rev.*, 1991, **91**, 165.
42 L. P. Hammett, *J. Am. Chem. Soc.*, 1937, **59**, 96.
43 A. R. Katritzky, M. Kuanar, S. Slavov, C. D. Hall, M. Karelson, I. Kahn and D. A. Dobchev, *Chem. Rev.*, 2010, **110**, 5714.
44 T. Kubota and H. Miyazaki, *Bull. Chem. Soc. Jpn.*, 1966, **39**, 2057.
45 M. N. Ackermann, K. B. Moore, A. S. Colligan, J. A. Thomas-Wohlever and K. J. Warren, *J. Organomet. Chem.*, 2003, **667**, 81.
46 J. E. Heffner, C. T. Wigal and O. A. Moe, *Electroanalysis*, 1997, **9**, 629.
47 N. Leventis, A. M. M. Rawaswdeh, G. H. Zhang, I. A. Elder and C. Sotiriou-Leventis, *J. Org. Chem.*, 2002, **67**, 7501.
48 M. L. Dell'arciprete, C. J. Cobos, J. P. Furlong, D. O. Martire and M. C. Gonzalez, *ChemPhysChem*, 2007, **8**, 2498.
49 K. Dedeian, P. I. Djurovich, F. O. Garces, G. Carlson and R. J. Watts, *Inorg. Chem.*, 1991, **30**, 1685.
50 S. Okada, K. Okinaka, H. Iwawaki, M. Furugori, M. Hashimoto, T. Mukaide, J. Kamatani, S. Igawa, A. Tsuboyama, T. Takiguchi and K. Ueno, *Dalton Trans.*, 2005, 1583.
51 J. Li, P. I. Djurovich, B. D. Alleyne, M. Yousufuddin, N. N. Ho, J. C. Thomas, J. C. Peters, R. Bau and M. E. Thompson, *Inorg. Chem.*, 2005, **44**, 1713.
52 B. D'Andrade, S. Datta, S. R. Forrest, P. Djurovich, E. Polikarpov and M. E. Thompson, *Org. Electron.*, 2005, **6**, 11.
53 I. Avilov, P. Minoofar, J. Cornil and L. De Cola, *J. Am. Chem. Soc.*, 2007, **129**, 8247.
54 E. Baranoff, B. F. E. Curchod, F. Monti, F. Steimer, G. Accorsi, I. Tavernelli, U. Rothlisberger, R. Scopelliti, M. Grätzel and M. K. Nazeeruddin, *Inorg. Chem.*, 2012, **51**, 799.
55 E. Baranoff, B. F. E. Curchod, J. Frey, R. Scopelliti, F. Kessler, I. Tavernelli, U. Rothlisberger, M. Grätzel and M. K. Nazeeruddin, *Inorg. Chem.*, 2012, **51**, 215.
56 A. J. M. Duisenberg, L. M. J. Kroon-Batenburg and A. M. M. Schreurs, *J. Appl. Crystallogr.*, 2003, **36**, 220.
57 R. H. Blessing, *Acta Crystallogr., Sect. A: Fundam. Crystallogr.*, 1995, **51**, 33.
58 G. M. Sheldrick, *Acta Crystallogr., Sect. A: Fundam. Crystallogr.*, 2008, **64**, 112.
59 A. A. Vlcek, E. S. Dodsworth, W. J. Pietro and A. B. P. Lever, *Inorg. Chem.*, 1995, **34**, 1906.
60 V. V. Grushin, N. Herron, D. D. LeCloux, W. J. Marshall, V. A. Petrov and Y. Wang, *Chem. Commun.*, 2001, 1494.
61 C. M. Cardona, W. Li, A. E. Kaifer, D. Stockdale and G. C. Bazan, *Adv. Mater.*, 2011, **23**, 2367.
62 V. V. Pavlishchuk and A. W. Addison, *Inorg. Chim. Acta*, 2000, **298**, 97.
63 Although equations are given with coefficients rounded to the closest 0.1, the coefficients have been all calculated from the results of the correlation, and not from the rounded numbers.
64 K. H. Lee, H. J. Kang, S. J. Lee, J. H. Seo, Y. K. Kim and S. S. Yoon, *Synth. Met.*, 2011, **161**, 1113.
65 R. Ragni, E. A. Plummer, K. Brunner, J. W. Hofstraat, F. Babudri, G. M. Farinola, F. Naso and L. De Cola, *J. Mater. Chem.*, 2006, **16**, 1161.
66 E. Baranoff, S. Suarez, P. Bugnon, H. J. Bolink, C. Klein, R. Scopelliti, L. Zuppiroli, M. Grätzel and M. K. Nazeeruddin, *ChemSusChem*, 2009, **2**, 305.
67 E. Baranoff, J. H. Yum, I. Jung, R. Vulcano, M. Gratzel and M. K. Nazeeruddin, *Chem.–Asian J.*, 2010, **5**, 496.
68 M. Marin-Suarez, B. F. E. Curchod, I. Tavernelli, U. Rothlisberger, R. Scopelliti, I. Jung, D. Di Censo, M. Gratzel, J. F. Fernandez-Sanchez, A. Fernandez-Gutierrez, M. K. Nazeeruddin and E. Baranoff, *Chem. Mater.*, 2012, **24**, 2330.
69 M. L. Xu, R. Zhou, G. Y. Wang and J. Y. Yu, *Inorg. Chim. Acta*, 2009, **362**, 2183.
70 I. S. Shin, S. Yoon, J. I. Kim, J. K. Lee, T. H. Kim and H. Kim, *Electrochim. Acta*, 2011, **56**, 6219.
71 J. Brooks, Y. Babayan, S. Lamansky, P. I. Djurovich, I. Tsyba, R. Bau and M. E. Thompson, *Inorg. Chem.*, 2002, **41**, 3055.
72 G. J. Zhou, Q. Wang, X. Z. Wang, C. L. Ho, W. Y. Wong, D. G. Ma, L. X. Wang and Z. Y. Lin, *J. Mater. Chem.*, 2010, **20**, 7472.
73 I. R. Laskar, S. F. Hsu and T. M. Chen, *Polyhedron*, 2006, **25**, 1167.
74 T. Sajoto, P. I. Djurovich, A. B. Tamayo, J. Oxgaard, W. A. Goddard and M. E. Thompson, *J. Am. Chem. Soc.*, 2009, **131**, 9813.
75 V. Sivasubramaniam, F. Brodkorb, S. Hanning, H. P. Loebl, V. van Elsbergen, H. Boerner, U. Scherf and M. Kreyenschmidt, *Cent. Eur. J. Chem.*, 2009, **7**, 836.
76 V. Sivasubramaniam, F. Brodkorb, S. Hanning, H. P. Loebl, V. van Elsbergen, H. Boerner, U. Scherf and M. Kreyenschmidt, *J. Fluorine Chem.*, 2009, **130**, 640.
77 I. R. de Moraes, S. Scholz, B. Lussem and K. Leo, *Org. Electron.*, 2011, **12**, 341.
78 S. J. Lee, K. M. Park, K. Yang and Y. Kang, *Inorg. Chem.*, 2009, **48**, 1030.
79 F. Kessler, R. D. Costa, D. Di Censo, R. Scopelliti, E. Ortí, H. J. Bolink, S. Meier, W. Sarfert, M. Grätzel, M. K. Nazeeruddin and E. Baranoff, *Dalton Trans.*, 2012, **41**, 180.
80 S. B. Meier, W. Sarfert, J. M. Junquera-Hernández, M. Delgado, D. Tordera, E. Ortí, H. J. Bolink, F. Kessler, R. Scopelliti, M. Grätzel, M. K. Nazeeruddin and E. Baranoff, *J. Mater. Chem. C*, 2013, **1**, 58.
81 F. O. Garces, K. A. King and R. J. Watts, *Inorg. Chem.*, 1988, **27**, 3464.

82 D. Tordera, M. Delgado, E. Ortí, H. J. Bolink, J. Frey, M. K. Nazeeruddin and E. Baranoff, *Chem. Mater.*, 2012, **24**, 1896.
83 S. M. W. Rahaman, S. Dinda, T. Ghatak and J. K. Bera, *Organometallics*, 2012, **31**, 5533.
84 K. I. Goldberg and A. S. Goldman, in *ACS Symposium Series 885*, American Chemical Society, Washington, DC, 2004.
85 B. Schmid, F. O. Garces and R. J. Watts, *Inorg. Chem.*, 1994, **33**, 9.
86 E. Baranoff, I. Jung, R. Scopelliti, E. Solari, M. Grätzel and M. K. Nazeeruddin, *Dalton Trans.*, 2011, **40**, 6860.
87 L. Rincon and R. Almeida, *J. Phys. Chem. A*, 2012, **116**, 7523.
88 S. S. Fielder, M. C. Osborne, A. B. P. Lever and W. J. Pietro, *J. Am. Chem. Soc.*, 1995, **117**, 6990.
89 H. Masui and A. B. P. Lever, *Inorg. Chem.*, 1993, **32**, 2199.